METRICA
METRology Institutional CAtalog

ISTITUTO NAZIONALE DI RICERCA METROLOGICA
Repository Istituzionale

A thermostatic chamber for doppler-broadening thermometry of mercury vapors

This is the author's accepted version of the contribution published as:

Original
A thermostatic chamber for doppler-broadening thermometry of mercury vapors / Lopardo, G., Bertiglia, F., Barbone, A., Bertinetti, M., Dematteis, R., Giraudi, D., Gianfrani, L.. - In: MEASUREMENT. - ISSN 0263-2241. - (2021), p. 108594. [10.1016/j.measurement.2020.108594]

Availability:
This version is available at: 11696/65263 since: 2023-06-07T14:06:45Z

Publisher:
Elsevier

Published
DOI:10.1016/j.measurement.2020.108594

Terms of use:

This article is made available under terms and conditions as specified in the corresponding bibliographic description in the repository

Publisher copyright

(Article begins on next page)

14 October 2026

A THERMOSTATIC CHAMBER FOR DOPPLER-BROADENING THERMOMETRY OF MERCURY VAPORS

G. Lopardo[1], F. Bertiglia[1], A. Barbone[1], M. Bertinetti[1], R. Dematteis[1], D. Giraudi[1], L. Gianfrani[2]

[1] *Istituto Nazionale di Ricerca Metrologica INRiM, Torino, Italy*
[2] *Department of Mathematics and Physics, Università degli Studi della Campania "Luigi Vanvitelli", Caserta, Italy*

corresponding author: Giuseppina Lopardo
E-mail: g.lopardo@inrim.it
address: Istituto Nazionale di Ricerca Metrologica - INRiM
Strada delle Cacce, 91
10135 Torino (Italy)

Abstract

We present an isothermal chamber designed and realized at the Italian Metrological Institute (INRiM) to stabilize the temperature of a quartz cell for Doppler-broadened precision spectroscopy of mercury atoms in the UV region for the practical realization of the new definition of kelvin. The challenge of this apparatus is the capability to control, with great accuracy, the temperature of a non-cylindrical quartz cavity containing the mercury vapors. The temperature was actively controlled and maintained stable within 0.05 mK at the triple point of water, for 15 hours, but longer periods are possible. The spatial uniformity was also characterized. The traceability of temperature measurements and the complete uncertainty budget are discussed.

Keywords: Doppler broadening thermometry, Isothermal chamber, Temperature metrology, Temperature control, Temperature stability, Uncertainty.

1. Introduction

On 20 May 2019 the kelvin, along with three other base units of the International System of Units (SI) [1], namely the kilogram, the ampere and the mole, has been redefined in terms of fundamental constants of nature [2]. In particular, the new kelvin is based on the Boltzmann constant. Starting from this definition, any method capable of deriving a temperature value traceable to the reference constant can, in principle, be used for its realization [3]. In practice, only few methods respond to the criteria set by the international temperature metrology community to realize a primary thermometer [4], among these, there is Doppler-Broadening Thermometry (DBT) [5].
The basic idea of DBT is to convert thermodynamic temperature determinations into frequency measurements [6]. So far, most of the DBT implementations have been performed on molecular samples, such as ammonia, water, carbon dioxide and acetylene, in the infrared portion of the electromagnetic spectrum [6]. In the last few years, big efforts have been done to bring DBT at the same level of accuracy of acoustic gas-thermometry and dielectric-constant gas thermometry [7, 8]. In particular, technical improvements of the setups have been accompanied by more and more refined models of the line shapes, to carefully take into account collisional effects [8].

An important ingredient for a successful DBT experiment is the choice of the spectral line, which must be well isolated to avoid any deformation of its profile due to collisional line mixing and quantum interference effects. This latter requirement can be more easily satisfied in an atomic vapor sample because of the simpler structure of the spectrum, as compared to molecular ones [9].

DBT can be effectively implemented in the deep-ultraviolet region by probing the 6^1S_0->6^3P_1 intercombination transition of the mercury bosonic isotopes. In fact, mercury (Hg) has a variety of favorable features for the aims of DBT. Its vapor pressure (equal to 0.026 Pa) at the triple point of water (TPW) temperature is several orders of magnitude larger than that of rubidium, potassium, or strontium. On the other hand, the pressure is small enough to completely neglect collisional perturbations to the line profile thus simplifying enormously the spectral analysis for temperature retrieval. Differently from the stable isotope of cesium, the possibility of probing a line with no hyperfine structure leads to a further simplification of the spectral analysis, in the Doppler-limited regime.

This paper describes the design and realization of the isothermal cell that will be used in an Hg-based DBT primary thermometer, currently under development within the framework of a National project. This system is fundamental for a successful experiment because temperature uniformity and stability directly affects the accuracy of the spectroscopic measurements. The novelty of this system is the extremely accurate control of temperature with a stability and uniformity better than 1 mK at the TPW, along with the direct traceability to the International Temperature Scale of 1990 (ITS-90) [10].
In literature are present different examples of thermostatic chamber for DBT. For a summary about the state of art and the level of temperature control see [11].
One of the differences between these systems and the chamber illustrated in this paper is in the gas holder to be thermalized. The new one is made of quartz instead of metal (generally stainless steel or aluminum) and presents a non-cylindrical geometry. These aspects have required to project a thermostatic system ad-hoc in order to afford the new thermal challenges. Indeed,

quartz is not a good conductor, as metal, and the presence of a capillary tube breaks the geometrical symmetry that helps to reduce spatial gradients.

The paper structure is the following: the mechanical design of the isothermal chamber is discussed in section 2.1. Section 2.2 gives the details about temperature control and measurement, as well as thermometers' calibration. Section 3 is dedicated to analyze the thermal characterization results, including the uncertainty budget. Finally, conclusions are drawn in section 4.

2. Material and methods

2.1 Thermostatic chamber

The Hg vapors are contained in a 20 mm long quartz cell (manufactured by Precision Glassblowing Inc.) sealed at the two ends by a pair of wedged AR-coated windows with diameter of 25.4 mm. A capillary tube, containing the mercury droplet, is welded in the middle of the cell, in the vertical direction, as shown in the left panel of Figure 1.

The isothermal chamber, expressly built to house the spectroscopic cell, consists of three components placed coaxially one inside the other:

1. a lathed copper cylinder acting as isothermal equalization block with an electrical heater wrapped around it;
2. an aluminum fluid heat exchanger;
3. an external vacuum chamber.

The quartz cell is enclosed in a cylindrical copper block with length and diameter of 90 mm, as shown in the right panel of Figure 1. The copper take care of temperature uniformity inside the cell to avoid Hg pressure variations related to thermal gradients. A coaxial cylindrical cavity in the block will allow the laser beam to pass through the cell. The block is divided in two parts in the middle, so as it is possible to open it and perfectly fit the capillary tube inside a hole drilled into the copper body in the transverse direction. Care was taken to reduce to a minimum the thermal decoupling between quartz and copper.

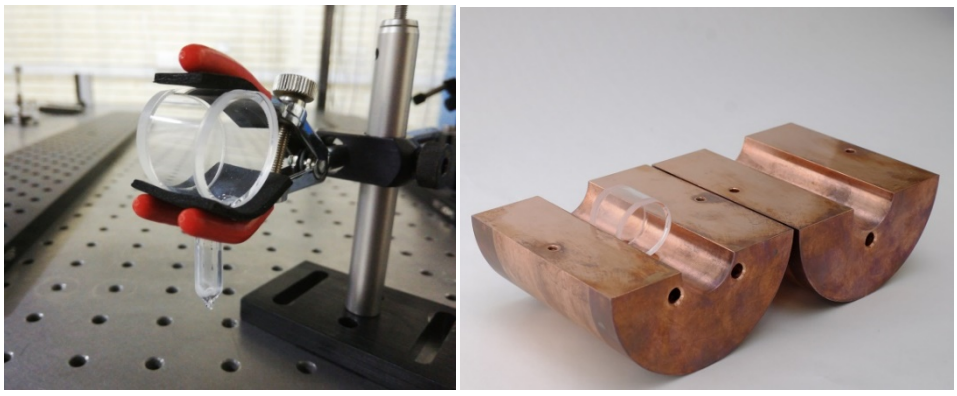

Figure 1: Quartz cell with mercury vapors, on the left; copper cylinder containing the quartz cell, on the right. (Figure in color only online)

Three thermometer wells were drilled, 70 mm deep, directly in the front side of the copper block with a displacement of 120° between them in order to detect any temperature non-uniformity inside it (Figure 2). Two capsule type Standard Platinum Resistance Thermometers (c-SPRTs), fitting perfectly the block, were inserted inside the wells. Both c-SPRTs (model 5686 manufactured by Hart Scientific) have a nominal resistance of 25.5 Ω at the TPW. One of them, designed HS144, is used to perform both temperature control and measurements, the other, designated HS156, to evaluate spatial uniformity.

A polyimide electrical heater, wrapped around the copper block (as shown in Figure 2), is used to provide a maximum of about 1 W heating power directly to the block.

Figure 2: copper cylinder with electrical heater wrapped around it,
and the thermometer wells labeled (Figure in color only online)

A silicone high vacuum grease was used to assure a good thermal contact between the components and the copper block.

The cooper block containing the Hg cell is inserted in an aluminum fluid heat exchanger, depicted on the left side of Figure 3. Two Teflon centering rings are used to keep the copper block in the horizontal position inside the exchanger and facilitate the extraction. The cylindrical symmetry has been used for all the components of the system to reduce any thermal asymmetry to a minimum.
The aluminum heater exchanger is formed by two concentric sealed vessels in which flows a thermostatic fluid. The fluid follows a defined path delimited by plates, in order to fill the whole volume and assure thermal uniformity.

Figure 3: Aluminum heater exchanger. A draw of interior, on the left; a photo of the exchanger holding the copper block, on the right. The electrical heater and the Teflon centering rings are visible. (Figure in color only online)

Finally, the exchanger containing the copper block and the Hg cell is suspended in a vacuum chamber by means of other Teflon centering rings. The vacuum chamber is a 334 mm long and 160 mm diameter stainless steel CF tees, closed by DN 160/40 CF flanges. Two optical glass windows are mounted on two sides of the vacuum chamber to allow laser incidence and transmission during DBT experiment. An external vacuum line connects the chamber to an oil-free scroll pump, and to a Pirani vacuum gauge to measure the vacuum pressure. The vacuum chamber has a twofold utility: thermal insulation of the spectroscopy cell from the external environment and the removal of moisture from the apparatus causing condensation on the structures and on the optical windows at temperatures below 0 °C.

2.2 Temperature control and measurement

Figure 4 shows a block diagram of the whole experimental system realized to control the temperature of the quartz cell.

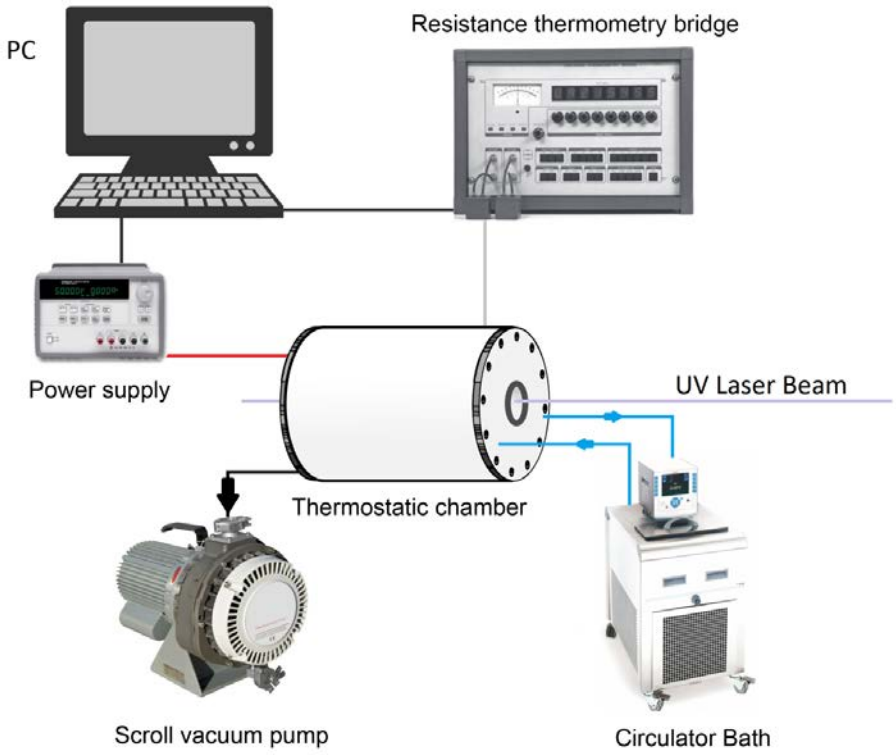

Figure 4: Block diagram of experimental set-up for thermostatic chamber characterization (Figure in color only online)

The temperature control is achieved by means of two independent control stages: the first one is driven by a commercial thermostat, and the second one by an electrical heater.
An external circulator bath (working range from -50 °C to +200 °C) cools the fluid flowing in the aluminum heat exchanger and brings the temperature of the cell 1 °C below the target temperature (0.01 °C). This difference was selected carefully to overcome thermostat fluctuations. In fact, higher differences have to be avoided since they would require excessive feed current for the fine control, while a smaller difference may increase the response time of the system.

The fine control of temperature is provided by the electrical heater around the copper block that is powered by a DC Power Supplies. A National Instrument LabVIEW Proportional-Integrative (PI) control drives the heater in term of voltage. The process variable is the temperature of the cell, and the set point is the TPW temperature. The PI controller determines the heater power, and applies the controller output value (the DC voltage) to the system in order to drive the process variable toward the set point value. The DC voltage could be varied between 0 V and 25 V, corresponding to a power ranging from 0.01 W to 4.28 W, but the maximum voltage of the PI control was limited to 12.5 V (1 W). So, stable working conditions were obtained and deep jumps between maximum and minimum values were avoided.

The process variable is measured by the HS144 c-SPRT and read by an Automatic System Laboratory (ASL) F18 primary-standard resistance bridge. Two LabVIEW programs-subroutines were developed for temperature measurements and control. In particular, the measurement software allows bridge reading, recording, and data saving. The control software, implementing the PI algorithm, allows automatic temperature control, manual heating, and temperature changes.
Instead, the external circulator bath temperature is fixed and not controlled by software.

The bridge reads the resistance ratio of the thermometer and a 25 Ω reference resistance calibrated at INRiM. The reference resistance is a standard resistor placed in its temperature-controlled enclosure.

The c-SPRTs were calibrated at INRiM in accordance to ITS-90 in the sub-range between -38.83 °C and 29.76 °C, namely, at the temperatures of the triple point of mercury, triple point of water and at the melting point of gallium [12]. In order to be inserted inside the fixed-point cells for calibration of long-stem SPRTs, each capsule thermometer was mounted within a copper sleeve embedded into a hollow stainless steel adaptor made at INRiM for this specific use. During calibration, the thermometer self-heating effect was evaluated.

3. Results and Discussion

3.1 Temperature stability and uniformity

Short and long term stability tests were performed in order to characterize the isothermal chamber. The short term test was carried out with the vacuum pump switched on, instead, the long term test was performed with the pump switched off. This allowed, also, to recognize possible differences between the two working conditions.

Figure 5 shows the temperature difference (T_c-T_{TPW}) between the temperature measured in chamber (T_c) and that evaluated during calibration at TPW (T_{TPW}) by HS144 c-SPRT. The record, 1 hour long (but longer period is possible), was carried out with a vacuum pressure in the chamber of $8.8*10^{-3}$ mbar (but higher pressure is possible). The temperature was kept stable within 0.025 mK, considering the standard deviation of the population as stability parameter [11]. These fluctuations, free of systematic effects, are of the same order of the instrument resolution.

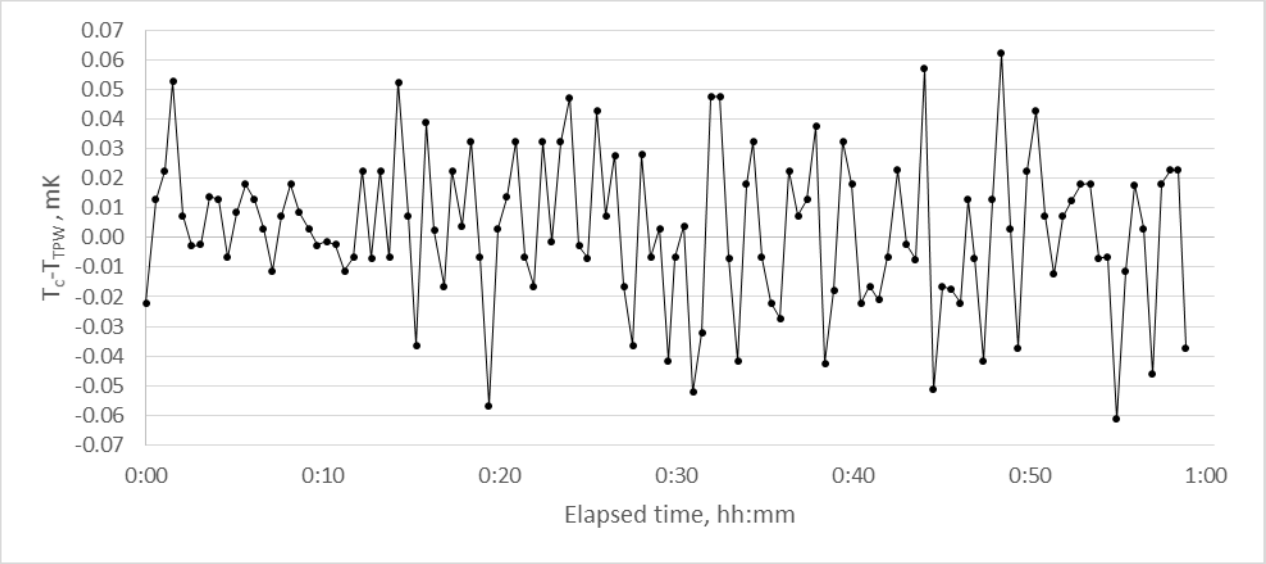

Figure 5: Temperature differences related to TPW for HS144 c-SPRT evaluated during 1 hour with vacuum pump switched on

Figure 6 reports the temperature difference (T_c-T_{TPW}) recorded during a longer time, 15 hours, at the end of which the control software was stopped manually. The mean difference is -0.02 mK and the standard deviation is 0.05 mK. These measurements were carried out with the vacuum pump switched off, after chamber evacuation.

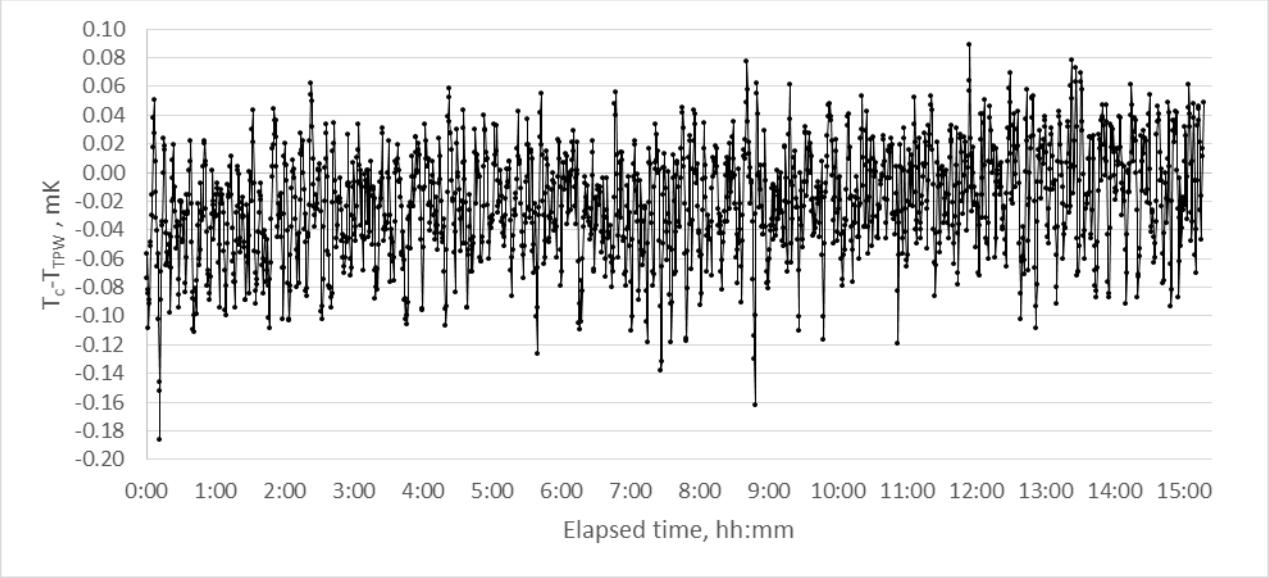

Figure 6: Temperature difference related to TPW for HS144 c-SPRT evaluated during 15 hours with vacuum pump off

As expected, with the pump off, there is a little drift of the data due to heat transfer from the outside. However, the stability evaluated in the two cases, pump switched on and off, is similar, so we can conclude that it will be possible to work successfully with the pump switched off to avoid any mechanical vibration that could perturb Doppler broadening measurements. Even though the vacuum chamber showed some leakage from tube inlets and cable connections (1 mbar per hour in static vacuum condition), the pressure increase didn't introduce perturbation of the system (below a certain value).

The spatial uniformity inside the isothermal chamber was evaluated comparing the temperature recorded by the both c-SPRTs located in two different positions inside the copper block. The HS144 was put inside the lower well near the capillary (well number 2 in figure 2) instead the HS156 in the upper well (well number 1 in figure 2). Table 1 reports the results obtained during four uniformity tests. *R(T)* is the mean resistance measured by each thermometer, T_c-T_{TPW} is the temperature difference related to TPW for each thermometer, and ΔT is the temperature difference measured between the two thermometers. The measurement number 3, showing a different behavior, may have been obtained in unstable conditions, but this had no impact on the magnitude of the thermal gradient.
The mean temperature difference measured was 7.1 mK, corresponding to a thermal gradient in the quartz cell of 0.92 mK/cm. This value was calculated dividing the mean value of ΔT by the distance between thermometers, and assuming a linear gradient of temperature in the copper.

Test n.	$R(T)$ HS156	$R(T)$ HS144	T_c-T_{TPW} for HS156	T_c-T_{TPW} for HS144	ΔT
1	25.344407 Ω	25.513415 Ω	7.04 mK	-0.15 mK	7.19 mK
2	25.344397 Ω	25.513416 Ω	6.95 mK	-0.14 mK	7.09 mK
3	25.344924 Ω	25.514055 Ω	12.16 mK	6.14 mK	6.02 mK
4	25.344500 Ω	25.513413 Ω	7.97 mK	-0.16 mK	8.14 mK
				Mean value	**7.1 mK**

Table 1: Spatial uniformity tests results

3.2 Uncertainty budget

Table 2 illustrates the various uncertainty contributions considered to obtain the uncertainty on temperature differences between the TPW temperature and those measured in the isothermal chamber. A simple linear model was adopted for the uncertainty estimation.

Uncertainty Source	u_i / mK	Probability distribution
Bridge (repeatability, non-linearity)	0.02	normal
Reference resistor stability	0.01	normal
Thermometer self heating	0.01	normal
Thermometer drift	0.04	normal
Chamber uniformity	0.53	rectangular
Chamber stability over 15 hours	0.05	normal
Temperature drift with pressure	0.02	rectangular
Combined Standard Uncertainty	0.54	

Table 2: Uncertainty budget for temperature differences between the TPW temperature and those measured in the chamber.

In rows 1 and 2 of table 2, the uncertainty contributions account for: the estimated repeatability and non-linearity of the F18 resistance bridge, and the effect of slight temperature variations of the standard resistor. The uncertainty sources in rows 3 and 4 are linked to the thermometer: the extrapolation to zero current of the resistance of c-SPRT (self-heating) and the thermometer drift between successive calibrations at the TPW

The chamber uniformity term was evaluated assuming a linear gradient inside the quartz cell. The recorded difference between the two c-SPRTs (0.92 mK/cm as reported in section 4.1) was weighted on the quartz cell length (20 mm) and the result was then divided by a factor *2sqrt(3*) considering a rectangular distribution of possible values.

The chamber stability contribution is equal to the standard deviation evaluated for 15 hours.

Finally, the uncertainty due to the drift of the temperature in the chamber in consequence of pressure increase, during 15 hours long test, was evaluated equal to 0.02 mK. This value was calculated considering a rectangular distribution. The total standard uncertainty is equal to 0.54 mK.

4. Conclusions

In order to develop and test a new primary gas thermometer based on Doppler-broadened precision spectroscopy of Hg atoms, an isothermal chamber was designed and realized. The adopted technical solutions have enabled to keep the temperature of a quartz cell, with mercury vapors, stable at the TPW temperature within 0.05 mK for 15 hours, in conditions of static vacuum. Longer periods are possible, especially if the vacuum pump is switched on. The temperature uncertainty was 0.54 mK, essentially due to the spatial gradient along the Hg cell.

Comparing our system with those reported by Wang et al. [11], a substantial improvement, among 1 order of magnitude, is observed in terms of temperature stability, either in the short- or in the medium- term, and overall standard uncertainty. The next step will be the integration of the

isothermal chamber into the laser spectrometer operating in the deep-ultraviolet, currently under development. The thermodynamic temperature of Hg atoms will be measured, first of all, at the TPW temperature where the Hg vapor pressure is suitable for spectroscopy measurements. After proving the potential of Doppler broadening thermometry on Hg vapors, the experiment will be extended to other ITS-90 fixed points. Determinations of the differences, T-T_{90}, between thermodynamic temperatures (T) provided by DBT and ITS's-90 temperatures (T_{90}), will be carried out and compared with values obtained with other primary techniques [13].

Acknowledgements

This work is being performed within the frame of a National project funded by the Italian Ministry for Education and Research, entitled "A new primary method of gas thermometry based upon Doppler-broadened mercury spectroscopy in the UV region" (MIUR, PRIN2015 Call, Project n. 20152MRAKH).The authors wish to thank Dr. Peter P. M. Steur for valuable discussions and advices.

References

[1] BIPM 2019 The new SI Brochure (9th edn.) https://www.bipm.org/utils/common/pdf/si-brochure/SI-Brochure-9.pdf , (accessed April 2020)

[2] M. Stock, R. Davis, E. de Mirandés, M. J T Milton, The revision of the SI—the result of three decades of progress in metrology, Metrologia 56 (2019) 022001,

[3] BIPM 2019 Mise en pratique for the definition of the Kelvin in the SI www.bipm.org/utils/en/pdf/si-mep/SI-App2-kelvin.pdf (accessed April 2020)

[4] J. Fischer, B. Fellmuth, C. Gaiser, T. Zandt, L. Pitre, F. Sparasci, M. D. Plimmer, M. de Podesta, R. Underwood, G. Sutton, G. Machin, R. M. Gavioso, D. Madonna Ripa, P. P. M. Steur, J. Qu, X. J. Feng, J. Zhang, M. R. Moldover, S. P. Benz, D. R. White, L. Gianfrani, A. Castrillo, L. Moretti, B. Darquié, E. Moufarej, C. Daussy, S. Briaudeau, O. Kozlova, L. Risegari, J. J. Segovia, M. C. Martín, D. del Campo, Metrologia **55** (2018), R1–R20

[5] G. Machin, Measurement Science and Technology 29 (2018), 022001

[-6] L. Gianfrani, Linking the thermodynamic temperature to an optical frequency: Recent advances in Doppler broadening thermometry, Philos. Trans. R. Soc. A: Math. Phys. Eng. Sci. 374, (2016), 20150047

[7] A. Castrillo, E. Fasci, H. Dinesan, S. Gravina, L. Moretti, L. Gianfrani, Optical Determination of Thermodynamic Temperatures from a C2H2 Line-Doublet in the Near Infrared, Phys. Rev. Applied 11, (2019) 064060

[8] R. M. Gavioso, D. M. Ripa, P. P. M. Steur, C. Gaiser,T. Zandt, B. Fellmuth, M. de Podesta, R. Underwood, G.Sutton, L. Pitre, F. Sparasci, L. Risegari, L. Gianfrani, A.Castrillo, and G. Machin, Progress towards the determination of thermodynamic temperature with ultra-low uncertainty, Philos. Trans. R. Soc. A: Math. Phys. Eng. Sci. (2016) 374, 20150046.

[9] G-W Truong, J D Anstie, E F May, T M Stace, and A N Luiten, Accurate lineshape spectroscopy and the Boltzmann constant, Nat. Comm. 6 (2015) 8345.

[10] Preston-Thomas H., The International Temperature Scale of 1990 (ITS-90). Metrologia 27, (1990) 3–10. doi:10.1088/0026-1394/27/1/002

[11] H. Wang, X. Wang, Y. Pan, B. Wang, and S. Yang, Thermostatic chamber for Doppler broadening temperature measurement", Proc. SPIE 11439, 2019 International Conference on Optical Instruments and Technology: Optoelectronic Measurement Technology and Systems, 114390I (2020). https://doi.org/10.1117/12.2542663

[12] P. Marcarino, P. P. M. Steur and R. Dematteis, Realization at IMGC of the ITS-90 fixed points from the argon triple point upwards, Temperature, its measurement and control in science and industry AIP Conf. Proc. 684 (2003) 65–70

[13] R. M. Gavioso, D. Madonna Ripa, P. P. M. Steur, R. Dematteis, D. Imbraguglio, Determination of the thermodynamic temperature between 236 K and 430 K from speed of sound measurements in helium, Metrologia 56 (2019) 045006

Figure Captions

Figure 1: Quartz cell with mercury vapors, on the left; copper cylinder containing the quartz cell, on the right. (Figure in color only online)

Figure 2: copper cylinder with electrical heater wrapped around it, and the thermometer wells labeled (Figure in color only online)

Figure 3: Aluminum heater exchanger. A draw of interior, on the left; a photo of the exchanger holding the copper block, on the right. The Teflon centering rings are visible. (Figure in color only online)

Figure 4: Block diagram of experimental set-up for thermostatic chamber characterization (Figure in color only online)

Figure 5: Temperature differences related to TPW for HS144 c-SPRT evaluated during 1 hour with vacuum pump switched on

Figure 6: Temperature difference related to TPW for HS144 c-SPRT evaluated during 15 hour with vacuum pump off